

MIT Open Access Articles

*Measuring and Reporting Electrical
Conductivity in Metal–Organic Frameworks: Cd*

The MIT Faculty has made this article openly available. *Please share*
how this access benefits you. Your story matters.

Citation: Sun, Lei et al. "Measuring and Reporting Electrical Conductivity in Metal–Organic Frameworks: Cd₂(TTFTB) as a Case Study." *Journal of the American Chemical Society* 138, 44 (November 2016): 14772–14782 © 2016 American Chemical Society

As Published: <http://dx.doi.org/10.1021/jacs.6b09345>

Publisher: American Chemical Society (ACS)

Persistent URL: <http://hdl.handle.net/1721.1/115124>

Version: Author's final manuscript: final author's manuscript post peer review, without publisher's formatting or copy editing

Terms of Use: Article is made available in accordance with the publisher's policy and may be subject to US copyright law. Please refer to the publisher's site for terms of use.



Measuring and Reporting Electrical Conductivity in Metal-Organic Frameworks: Cd₂(TTFTB) as a Case Study

Lei Sun, Sarah S. Park, Dennis Sheberla, and Mircea Dincă*

Department of Chemistry, Massachusetts Institute of Technology, 77 Massachusetts Avenue, Cambridge, Massachusetts 02139, United States

ABSTRACT: Electrically conductive metal-organic frameworks (MOFs) are emerging as a subclass of porous materials that can have a transformative effect on electronic and renewable energy devices. Systematic advances in these materials depend critically on the accurate and reproducible characterization of their electrical properties. This is made difficult by the numerous techniques available for electrical measurements and the dependence of metrics on device architecture and numerous external variables. These challenges, common to all types of electronic materials and devices, are especially acute for porous materials, whose high surface area make them even more susceptible to interactions with contaminants in the environment. Here, we use the anisotropic semiconducting framework Cd₂(TTFTB) (TTFTB⁴⁻ = tetrathiafulvalene tetrabenzoate) to benchmark several common methods available for measuring electrical properties in MOFs. We show that factors such as temperature, chemical environment (atmosphere), and illumination conditions affect the quality of the data obtained from these techniques. Consistent results emerge only when these factors are strictly controlled and the morphology and anisotropy of the Cd₂(TTFTB) single crystal devices are taken into account. Most importantly, we show that depending on the technique, device construction, and/or the environment, a variance of one or even two orders of magnitude is not uncommon for even just one material if external factors are not controlled consistently. Differences in conductivity values of even two orders of magnitude should therefore be interpreted with caution, especially between different research groups comparing different compounds. These results allow us to propose a reliable protocol for collecting and reporting electrical properties of MOFs, which should help improve the consistency and comparability of reported electrical properties for this important new class of crystalline porous conductors.

Introduction

Long considered insulators par-excellence, metal-organic frameworks (MOFs)¹ are emerging as a remarkably tunable class of porous conductors. With electrical conductivity adding a new dimension to their tunable nature, MOFs have found new applications in electronic devices² such as chemiresistive sensors,^{3,4} batteries,⁵⁻⁹ supercapacitors,^{10,11} photovoltaics,¹² thermoelectrics,¹³ and field-effect transistors.^{14,15} These complement their more traditional uses in gas adsorption,^{16,17} gas separation,¹⁸ catalysis,^{19,20} or sensing.²¹ Advances in these new areas depend critically on benchmarking the electrical properties of MOFs, including electrical conductivity, charge mobility, charge density, electronic band gap, and charge activation energy, for instance. In a recent review on the topic of electrically conductive MOFs, we pointed out the relative lack of information regarding these fundamental electrical properties. We argued that the relative lack of data stems primarily from inconsistent usage of various techniques.²² These inconsistencies make comparisons between various frameworks difficult at best. Most often, such comparisons are uninformative. With the pace of new reports in this area accelerating, it is imperative that a set of rigorous guiding principles for electrical measurements become available to the community, lest inconsistent reports and techniques will negatively impact the systematic discovery

process. In this article, we use the semiconducting MOF Cd₂(TTFTB) (TTFTB⁴⁻ = tetrathiafulvalene tetrabenzoate)²³ to show that the observed electrical conductivity of MOFs depends on the physical form, crystallographic direction, temperature, atmosphere, and illumination conditions, among a host of other factors. With these results, we develop and propose a set of guidelines for reporting electrical conductivity, with the intention to improve the consistency and comparability between existing and future reports of electrically conductive MOFs.

As described previously,²³ TTF moieties in Cd₂(TTFTB) form one-dimensional infinite helical π -stacks with 6_s symmetry, which are responsible for anisotropic charge transport along the crystallographic c axis. The TTF stacks run parallel to infinite cadmium-carboxylate chains formed by benzoate groups connected to the TTF cores (Figure 1a and 1b). The benzoate groups also delineate one-dimensional cylindrical pores with a van der Waals diameter of ~ 5 Å, which give rise to a surface area of 559 m²/g. Because of the anisotropic structure, the electrical conductivity of Cd₂(TTFTB) along the c axis ($\sigma_{\parallel c}$, the direction of TTF stacks) is expected to be higher than that perpendicular to the c axis ($\sigma_{\perp c}$), a hypothesis that we probe below. Single crystals of Cd₂(TTFTB) are typically hexagonal rods (Figure 1c and 1d) that can reach 3 mm in length. Crystal indexing showed that the long dimension of the crystal indeed

coincides with the crystallographic c axis of $\text{Cd}_2(\text{TTFTB})$ (Figure S1). Previous measurements on 22 single crystals of $\text{Cd}_2(\text{TTFTB})$ from 4 independent synthetic batches performed by pasting two gold wires onto the hexagonal faces of the rods revealed an average electrical conductivity $\sigma_{\parallel c} = 2.86 (\pm 0.53) \times 10^{-4} \text{ S/cm}$. The electrical conductivity of $\text{Cd}_2(\text{TTFTB})$ did not change after exposure to air for at least 4 months, indicating that the framework does not degrade under ambient conditions during this period.

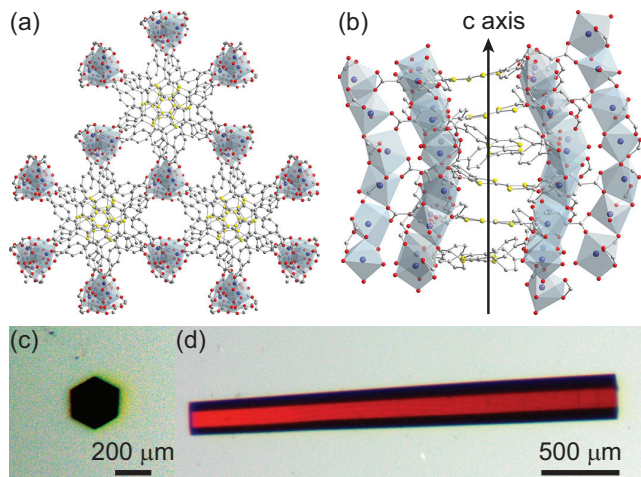


Figure 1. Portions of the X-ray crystal structure of $\text{Cd}_2(\text{TTFTB})$: (a) view along the c axis; (b) view along the ab plane showing a portion of the helical TTF stacks parallel to the c axis. Optical images of single crystals of $\text{Cd}_2(\text{TTFTB})$: (c) along the c axis showing the hexagonal cross section, (d) along the ab plane showing the long dimension of the hexagonal rod under polarized light. Blue, yellow, red, and grey spheres represent Cd, S, O, and C atoms, respectively. H atoms and solvent molecules were omitted for clarity.

Given its stability, anisotropy, crystal habit, and moderate electrical conductivity, we deemed $\text{Cd}_2(\text{TTFTB})$ to be a good choice for studying the impact of measurement technique and environment on the electrical conductivity of MOF single crystals. The stability of $\text{Cd}_2(\text{TTFTB})$ in air eases device fabrication and characterization. The moderate electrical conductivity enables the use of both 2- and 4-contact probe methods (*vide infra*), while minimizing the requirements imposed on the sensitivity of ammeters and voltmeters used in the measurements. The expected anisotropy for electrical conduction enables us to illustrate techniques for measuring electrical conductivity along different directions. The large size and relative mechanical strength of the crystals allow us to utilize the more technically challenging 4-contact probe method (*vide infra*). The regular hexagonal shape of the crystal leads to an accurate calculation of the area of the contacts cross section. Finally, the porosity and the semiconductor nature of $\text{Cd}_2(\text{TTFTB})$ illustrate the impact of environmental variables on the electrical conductivity.

Here, we first introduce the theoretical background of methods for measuring electrical conductivity of materials in general. We then discuss practical details of measuring pressed pellets and single crystals of $\text{Cd}_2(\text{TTFTB})$ and use the experimental results to compare all of these methods. We also discuss the influence of temperature, atmosphere, and illumination on the electrical conductivity of $\text{Cd}_2(\text{TTFTB})$. We do not describe the

electrical conductivity measurements of thin films in this article. Details for fabrication techniques, such as lithography, deposition, and etching, that are widely used for inorganic and organic semiconductors are readily available.²⁴ However, researchers must be careful when adapting these techniques to MOFs because these materials may not survive the experimental conditions required to implement some of these techniques, such as high vacuum, high temperature, strong acid or basic solution, high-power plasma, etc. When such techniques are employed, we recommend that the integrity of the MOF samples be confirmed by standard (powder) diffraction experiments.

Methods for measuring electrical conductivity

Electrical conductivity, σ , measures a material's ability to conduct electrical current. Measuring σ typically requires incorporating the material of interest into an electronic device, typically a resistor, and measuring the electrical conductance (G), length (L), and cross-sectional area (A) of the conduction channel.

$$\sigma = G \frac{L}{A} = \frac{I}{V} \times \frac{L}{A} \quad (1)$$

The electrical conductance is generally obtained by fitting the linear region of a current-voltage (I-V) curve to Ohm's law. Depending on the nature of the material, charge transport may be limited by contacts at low voltage²⁵ or may fall into space charge limited current regime at high voltage,²⁶ both of which lead to a nonlinear I-V curve. Therefore, the appropriate voltage or current range is typically determined by experiment. The measured electrical conductance is determined by the intrinsic electrical conductivity of the material, but is also dependent on the crystallinity and physical form of the measured sample, direction of electrical conduction, device quality, environment, leakage current, and the sensitivity of the ammeter and voltmeter. Equally important are the length and cross-sectional area of the conduction channel, which can be difficult to measure accurately and often introduce systematic errors, especially if the shape of the conduction channel is irregular.

Clearly, accurate measurements of intrinsic electrical conductivity are challenging and fraught with potential sources of errors. For these reasons, many methods have been developed to measure electrical conductivity.^{24,27,28} In this article, we focus on 2-contact probe, 4-contact probe, 4-point probe, and van der Pauw methods (Figure 2), the most common and accessible methods that will likely be of use to synthetic chemists in this field. The relevant equations that allow the measurement of conductivity in 2-contact and 4-contact probe methods are based on equation 1. In the 2-contact probe method, the sample is usually cut into a bar/rod-like shape, where two opposite surfaces are connected to thin metal wires (gold or copper wires with diameter of $10 \sim 100 \mu\text{m}$) by conductive adhesive paste (silver, gold, or carbon paste) (Figure 2a). Voltage or current is supplied or measured through the two wires. This method measures the total resistance of the sample, contacts, and wires. Because the equivalent circuit represents a number of resistors in series (Figure 2e), the resistance of the sample must be significantly larger than the total resistance of the contacts and the wire leads, which thus need not be known precisely. The typical resistance of wires and contacts is less than 100Ω . Therefore, to measure electrical conductivity with less than 10% error, the resistance of the sample needs to be higher than $1 \text{ k}\Omega$.

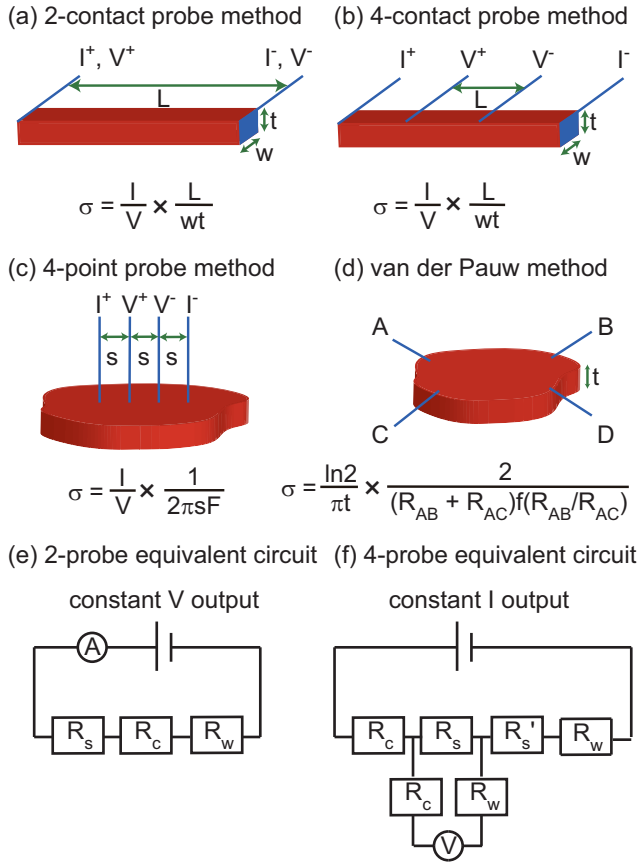


Figure 2. Methods for measuring electrical conductivity of MOFs (a to d). Red and blue areas represent samples and electrodes, respectively. I: current; V: voltage; L: sample length; w: sample width; t: sample thickness; s: distance between adjacent probes; σ : electrical conductivity; F and $f(R_{AB}/R_{AC})$: correction factors; +: input; -: output. (e) Equivalent circuit for a 2-contact-probe device. (f) Equivalent circuit for 4-contact-probe, 4-point-probe, and van-der-Pauw devices. R_s : resistance of sample of interest; R_c : contact resistance; R_w : wire resistance; R_s' : sample resistance that is not measured; A: ammeter; V: voltmeter.

If the resistance of the sample is comparable to or smaller than the total resistance of the contacts and wires, the 4-contact probe method should be used. In this method, four in-line probes are connected to the sample (Figure 2b). The outer two probes supply current, while the inner two probes measure voltage. The equivalent circuit for this configuration consists of contact and wire resistors in series with a voltmeter, both parallel to the sample resistor (Figure 2f). This circuit eliminates contact and wire resistances and measures only the resistance of the sample as long as it is significantly smaller than the internal resistance of the voltmeter, typically on the order of teraohms to petaohms. This assumption is justified even for poorly conducting samples with resistances exceeding 1 G Ω . This method thus allows for an accurate determination of electrical conductivity that does not depend on the resistance of the wires or contacts. The same method can of course be applied to highly resistive samples, although measurements of σ with 4-contact or 2-contact probe techniques for highly resistive materials should naturally give nearly identical results.

Whereas the 2- and 4-contact probe techniques are ideal for single crystals, the 4-point probe and van der Pauw methods are the most appropriate for measuring the electrical conductivity of irregularly shaped samples. As with the 4-contact probe method, both the 4-point probe and van der Pauw methods eliminate contributions from the resistance of contacts and wires (Figure 2f). In the former, four small (i.e. point-like) probes are placed linearly onto the surface of the sample, making point contacts (Figure 2c). The probes typically consist of pre-aligned equidistant metal pins. The equal spacing between the pins simplifies the probe operation and afferent calculations. Current is supplied through the outer two probes, while voltage is measured through the inner two probes. Importantly, this technique assumes that the sample size is infinite both laterally and vertically, that the contacts between the four point-probes and the sample are infinitesimally small, and that the sample exhibits isotropic conductivity. Practically, these assumptions are difficult to meet, and a correction factor (F) is applied to evaluate the electrical conductivity:

$$\sigma = \frac{1}{2\pi s F} \times \frac{I}{V} \quad (2)$$

F corrects for lateral sample dimensions, sample thickness, and placement of the probes relative to the sample edges, among others. The various corrections convoluted within F are detailed in reference 27.

The van der Pauw method is better suited for thin samples, such as thin films, which deviate considerably from the assumption of infinite thickness implicit in the 4-point probe technique.^{29,30} In the van der Pauw method, four point contacts are placed at the circumference of a sample to define a square (Figure 2d). One of the requirements here is that the surface roughness of the sample must be significantly smaller than the thickness, t , to reduce the error in thickness estimation. Two probes defining one edge of the square supply current, while two probes at the opposite edge measure voltage. As shown in Figure 2d, two orthogonal resistances are measured: $R_{AB} = V_{CD}/I_{AB}$, $R_{AC} = V_{BD}/I_{AC}$. Under this notation, R_{AB} is measured by passing current between point contacts A and B and measuring the voltage between contacts C and D (Figure 2d). The second resistance, R_{AC} , is determined in a similar manner. The electrical conductivity is calculated based on these two resistances and the thickness of the sample:

$$\sigma = \frac{\ln 2}{\pi t} \times \frac{2}{(R_{AB} + R_{AC}) f(R_{AB}/R_{AC})} \quad (3)$$

Here, $f(R_{AB}/R_{AC})$ is a function of the ratio between R_{AB} and R_{AC} :

$$\frac{R_{AB}/R_{AC} - 1}{R_{AB}/R_{AC} + 1} = \frac{f(R_{AB}/R_{AC})}{\ln 2} \text{COSH}^{-1} \left(\frac{\exp[\ln 2 / f(R_{AB}/R_{AC})]}{2} \right) \quad (4)$$

Details on the meaning and provenance of $f(R_{AB}/R_{AC})$ are found in reference 27.

The four methods described above and summarized in Figure 2 are widely used to measure electrical conductivity in metals and classical semiconductors. Here, we adapt these methods to MOFs and show, using Cd₂(TTFTB) as a case study, that they all give reasonable results when the implicit assumptions and potential pitfalls are treated appropriately.

Techniques for measuring pressed pellets of MOFs

Pressed pellets are made by compressing crystallites of a given material under a certain pressure, which improves the

contact between neighboring crystallites. Pressed pellets are accessible for most solid-state materials, and are advantageous because their size is often larger than that of single crystals, which simplifies the device fabrication process. Although all four methods discussed above are applicable to pressed pellets, the grain boundaries in pressed pellets introduce a large bulk resistance, which increases with the size of the pellet. The most important consequence of the grain boundaries is that for conductive samples (i.e. those whose intrinsic resistance is lower than the grain boundary resistance), the intrinsic conductivity cannot be determined from pressed pellet measurements. Indeed, in such cases, grain boundaries entirely dominate the observed bulk conductivity, which can be much lower than the intrinsic conductivity. Because the pressure at which a pellet is pressed, the relative size of the crystallites, and the relative orientation of the crystallites within the pellets all greatly influence the grain boundary resistance, conductivity values measured in pressed pellets can be unreliable and poorly reproducible. Furthermore, the random orientation of crystallites in pressed pellets (Figure 3e) implies that, for materials exhibiting anisotropic conduction, the observed bulk conductivity of a pellet is a weighted average of the electrical conductivity in each crystallographic direction (σ_{average}). Finally, the pressure applied in the preparation of pellets can itself cause phase transformations and, particularly relevant for MOFs, material degradation through framework collapse. Because of these disadvantages, pressed pellets should be employed in electrical measurements only when single crystals are not accessible or when device fabrication using single crystals is particularly challenging.

With these caveats in mind, we tested the reliability of pressed pellet measurements with $\text{Cd}_2(\text{TTFTB})$ using all four methods described above. Pellets were pressed at a pressure of approximately 200 MPa with the *in situ* press approach or 1 GPa with other approaches (*vide infra*). Electrical measurements were performed at a constant temperature of 297 K, in air with a relative humidity of 35% ~ 46%, and in the absence of light. Powder X-ray diffraction analysis of the pellets confirmed that compression under these conditions and electrical measurements did not affect the structure of $\text{Cd}_2(\text{TTFTB})$ (Figure S2). Details on device fabrication, electrical characterization, and calculations of electrical conductivity for these pellets can be found in the Supporting Information.

Results from 2-contact and 4-contact probe measurements on pressed pellets

The classical means to implement the 2-contact probe method is to cut a pellet into a parallelepiped shape and attach two wires onto two opposite faces using a conductive paste, an approach that we refer to as the “wire-paste approach”. The same device can be turned into a 4-contact probe device if two additional wires are pasted between the original two (see Figure 3a, b). The electrical conductivity can be calculated from equation 1 with parameters shown in Figure 2a and 2b. Subjecting a pellet of $\text{Cd}_2(\text{TTFTB})$ to this procedure, both 2- and 4-contact-probe devices were measured on the same sample, giving electrical conductivity values of 2.29×10^{-6} S/cm and 4.08×10^{-6} S/cm, respectively. The consistency between the two methods suggested that the total resistance of contacts and wires was negligible compared to the resistance of the pellet.

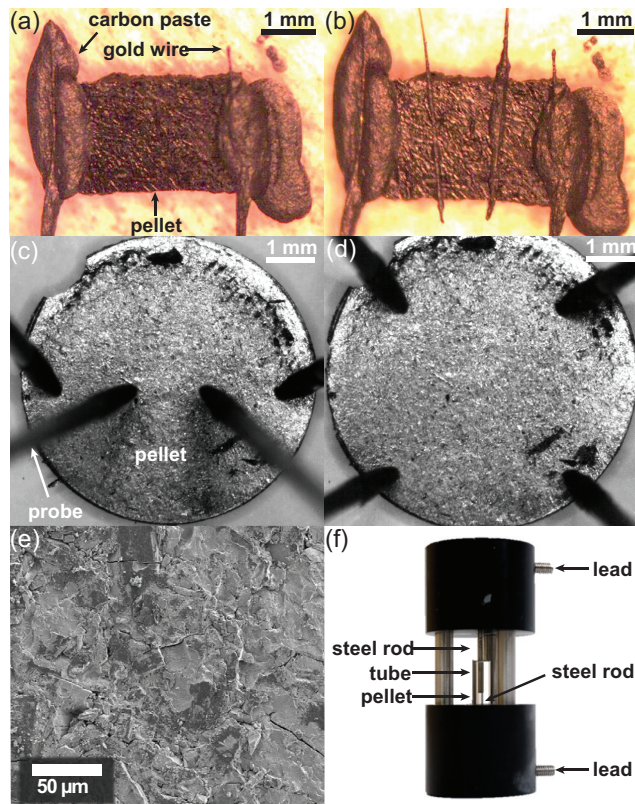


Figure 3. Devices made from $\text{Cd}_2(\text{TTFTB})$: (a) A pressed pellet, 2-contact-probe device made by the wire-paste approach. (b) A pressed pellet, 4-contact-probe device made by the wire-paste approach. (c) A pressed pellet, 4-point-probe device made by the direct-contact approach. (d) A pressed pellet, van der Pauw device made by the direct-contact approach. (e) Scanning electron micrograph of a pressed pellet. (f) Home-built apparatus for fabricating and measuring 2-contact-probe pressed pellet devices *in situ*.

The wire-paste approach imposes certain mechanical requirements on materials: the pellets must be sufficiently mechanically robust to survive the cutting process, and the obtained parallelepipeds should have relatively smooth surfaces for accurate calculation of the cross-sectional area where the paste is applied. Finally, depending on the formulation of the conductive paste, drying of this paste can cause pellets to crack due to strain. Because the conduction channel is often irregular (see Figure 3a, b), equation 1 is not directly applicable, and additional analysis is required to account for the geometry of the channel. These analyses, as applied to $\text{Cd}_2(\text{TTFTB})$ devices shown in Figure 3a and 3b, is described in detail in the Supporting Information. It is important to realize that these difficulties affect device fabrication from pellets and introduce errors in the determination of electrical conductivity that are often difficult to eliminate.

Some of the difficulties associated with pressing and cutting large pellets and fabricating devices from them can be alleviated by employing a simple home-built 2-contact-probe apparatus for very small pressed pellets, which we adopted from a reported setup that can be easily manufactured.³¹ As shown in Figure 3f, this simple apparatus consists of two plastic-supported stainless steel rods and a glass tube. The diameter of the rods and the inner diameter of the tube are the same, 0.208 cm

in our setup. The small diameter of the tube allows measurements of small amounts of sample, with reproducible measurements routinely obtained from approximately 2 mg. Thus, a given sample is introduced into the tube, and pressed into a dense pellet by the two rods, which also create direct electrical contacts that do not require additional conductive paste. If the electrical contact is inadequate, a layer of carbon-coated aluminum foil between rods and the sample can improve contact. The resulting pellet is a circular plate, whose thickness (0.1 ~ 1 mm) and area (0.0340 cm²) are well defined and can be easily measured, making the calculation of electrical conductivity simple and accurate. Therefore, this “*in situ* press” equipment provides convenient, quick, and accurate characterization of electrical conductivity of pressed pellets. Because of its simplicity and ease of handling, it can readily be adapted to inert environments, such as in glove boxes, to allow measurements of air-sensitive materials. With this method, we measured 9 pressed pellets of Cd₂(TTFTB) with various thickness (170 ~ 820 μm), obtained a linear relationship between the electrical conductivity and the thickness of pellets (Figure S4), and extracted an average electrical conductivity of $2.07 (\pm 0.13) \times 10^{-6}$ S/cm based on equation 1. This is comparable with the values obtained from the wire-paste approach, again highlighting the fact that contact resistances influence only minimally the total resistance of the sample.

4-point probe method and van der Pauw method

The 4-point probe and van der Pauw methods physically eliminate the influence of contact resistances. With these, the quality of the contacts does not significantly affect the measurements. The creation of cracks upon drying notwithstanding, 4-point-probe and van der Pauw devices can therefore be constructed using the relatively rudimentary wire-paste approach. In practice, however, pasting 4 parallel equidistant wires with point contacts on the same pellet is difficult. To address this challenge, we developed a “direct contact” method. Here, we employ a probe station equipped with four micro-manipulated arms (Figure S3) to land four metallic probes onto the surface of a pellet in either linear or square configurations (Figure 3c and 3d). A calibrated optical monoscope ensures linear and equidistant alignment of the probes for the 4-point probe method as well as square alignment of the probes for the van der Pauw method. This method gave 4-point-probe and van der Pauw conductivities of 4.39×10^{-6} S/cm and 2.70×10^{-6} S/cm, respectively, again in-line with the value obtained by the previous methods, confirming that contact resistances are negligible for pellets of Cd₂(TTFTB).

Techniques for measuring single crystals of MOFs

Single crystals present the ideal morphology for studying the intrinsic electrical conductivity of materials. They have few grain boundaries and defects, and allow the measurement of anisotropic properties should these be expected. The main challenges of working with single crystals, especially for MOFs, are their small size (often less than 200 μm) and their brittleness. Indeed, without practice it can be challenging to paste four (or even two) thin metal wires onto a 200 μm-long crystal while avoiding short-circuiting the leads. As with pellets, contacting the crystals directly with the relatively hard wires can often break the crystal, whereas using conductive paste can short-circuit the device or break the crystal upon drying.

General considerations for device fabrication

In principle, 2-contact probe, 4-contact probe, 4-point probe, and van der Pauw methods are all applicable to single crystals. However, due to the small size of single crystals of MOFs (< 1 mm), methods involving 4 contacts can be challenging. As such, the two-contact probe method is the most practical because it can be implemented with crystals as small as a few tens of microns. However, one should keep in mind that *the 2-contact probe method is not applicable to conductive samples* whose resistance is less than 1 kΩ, such as several reported two-dimensional MOFs.^{15,32–34} Using this method for samples that are too conductive will greatly underestimate the conductivity.

Because most MOFs are grown from solution, crystals often vary in size, shape, purity, number of defects, and surface quality from one batch to another or even within the same batch. In addition, different single-crystal device fabrication processes give rise to different electrode-crystal interfaces, charge injection efficiencies, and crystal-substrate interfaces, which vary even in the devices fabricated by the same technique. These factors may all affect the measured electrical conductivity. Therefore, *single-crystal electrical conductivity measurements should never be reported in isolation*, and multiple measurements should be executed to obtain sufficient statistics and minimize the standard deviation. Indeed, reporting conductivity from just one single crystal may lead to misinterpretation of the electrical conductivity. We recommend that average values obtained from at least three single crystals from at least three different batches, respectively, accompany reports of “champion” results from the best single-crystal devices. A few obvious considerations should also be followed when selecting any single crystal for conductivity measurements: the crystal should have appropriate length for the chosen device, a regular shape to simplify measuring the length of the conduction channel and cross-sectional area, and should be free of visible microcracks. Although such microcracks may not affect crystal quality with respect to X-ray diffraction, they act as grain boundaries that increase resistance, and act as weak spots that may lead to larger cracks and device failure under operational conditions. Crystals of Cd₂(TTFTB) used for this study were at least 100 μm long and were essentially free of visible cracks as determined by optical microscopy. All crystals had a hexagonal rod habit, which facilitates fabrication of 2-contact-probe devices. Irregularly shaped crystals will require certain mathematical models to estimate the length and the cross-sectional area of the conduction channel in 2-contact-probe or 4-contact-probe devices (see the mathematical models used for 2-contact-probe and 4-contact-probe devices of pressed pellets in Supporting Information). Plate-like crystals are particularly well suited for the van der Pauw method.

One important consideration for fabricating single-crystal devices with conductive paste is the choice of paste.²⁸ The mechanical strength and the viscosity of the paste should be able to support permanent contacts. The hydrophilicity of the paste should match that of the sample so that the paste can wet the sample to provide good contact. If the sample is a semiconductor, the work function of the conductive paste should be aligned with that of the sample to eliminate potential Schottky barriers and ensure Ohmic contacts. In particular, the work function of the conductive paste should be lower than that of an n-type material and higher than that of a p-type material.³⁵ Satisfying this

requirement may be challenging because the work function and the charge carrier type of the material of interest are generally unknown. In practice, increasing the contact area between the crystal and the electrode by using rough surfaces or creating asperities at the crystal-electrode interface both help facilitate charge injection and the formation of Ohmic contacts.³⁵ More specifically for MOFs, the paste should be sufficiently viscous so that it is not absorbed into the MOF pores. Additionally, one should consider the chemical compatibility between the MOF and the paste. For instance, one should not use silver paste for an I₂-doped material because this may lead to the formation of insulating AgI at the interface.²⁸ Finally, one should also confirm the stability of the sample in the solvent used to formulate the conductive paste (i.e. water, isopropanol, certain polymers, etc.). In our hands, Ag paste led to mostly non-linear I-V curves even in the low voltage regime, whereas carbon-based pastes led to ohmic I-V behavior with crystals of Cd₂(TTFTB). The results described herein are those obtained with carbon paste-based devices.

Another important consideration when measuring electrical properties is the choice of underlying substrate used to assemble the device. Naturally, the substrate must be considerably more insulating than the sample so that the leakage current is negligible. With an electrical conductivity of 10⁻¹¹ ~ 10⁻¹⁵ S/cm at 300 K, dry glass is sufficiently insulating to serve as substrate for measuring metals and semiconductors. Quartz, sapphire, and Teflon are even more insulating than glass and are thus appropriate substrates for insulators. For very insulating materials, only vacuum is sufficiently insulating to qualify as an appropriate substrate. Furthermore, when performing variable-temperature electrical conductivity measurements, one should choose electrically insulating and thermally conductive substrates, such as sapphire, that allow efficient heat transfer between the sample and the heating/cooling system. Adding a layer of thermally conductive (but electrically insulating) paste between the sample and the substrate can also assist with heat transfer.

Results discussed below for single crystals of Cd₂(TTFTB) follow the guidelines described above. Single-crystal devices were fabricated by various approaches that are introduced below. Devices were fabricated manually, with micro-manipulators, or with standard lithography techniques. The facilities used for device fabrication are typically accessible in semiconductor laboratories or commercially available. All measurements were performed at 297 K, in air with relative humidity of 30% ~ 50%, and in the absence of light. Details on device fabrication and electrical characterization can be found in the Supporting Information.

Results for Cd₂(TTFTB) single crystals from the wire-paste approach

The wire-paste approach is the most popular for fabricating single-crystal devices of organic crystals. It consists of attaching two or four metal wires manually, using a conductive paste, to a single crystal resting on an insulating substrate. The wires are anchored on the substrate by conductive paste or wire bonding, and finally the device is connected to electronic instruments by touching the paste or metal pads with wires or probes (Figure 4a).

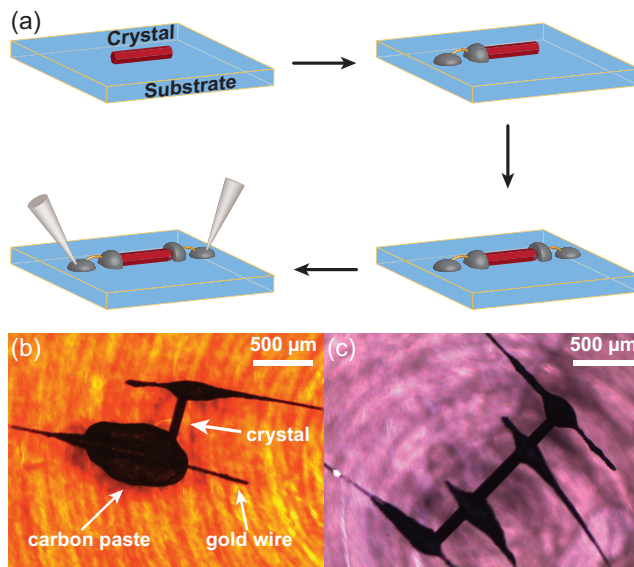


Figure 4. (a) Fabrication scheme of a 2-contact-probe device made from a single crystal of Cd₂(TTFTB) using the wire/paste approach. Optical images of 2- and 4-contact-probe single-crystal devices are shown in (b) and (c), respectively.

We measured 25 two-contact-probe single crystal devices made from four independently synthesized batches of Cd₂(TTFTB) (Figure 4b). The average conductivity over all these devices was $2.51 (\pm 0.46) \times 10^{-4}$ S/cm. We also fabricated one four-contact-probe device (Figure 4c), which gave a conductivity of 1.91×10^{-4} S/cm. The similarity between the two- and four-contact-probe conductivity values indicates that the contact resistance at the interface between carbon paste and the crystal is negligible compared with the resistance of the crystal. The two-contact probe method is therefore sufficiently accurate for all subsequent measurements. In all cases, the two hexagonal ends of the rod-like crystals were fully covered in conductive paste, ensuring that the conductivity measured was that along the crystallographic *c* axis, the direction of the TTF stacks, giving σ_{\parallel} .

The wire-paste approach does not require sophisticated and expensive probe positioning instruments, and provides mechanically stable devices that can be used at various temperatures, in vacuum, or in various atmospheres. However, manually attaching wires to small crystals (i.e. < 200 μm in length) requires practice.

Probe-paste approach

When crystals are too small to be handled reliably and comfortably by hands, contacts may be attached using micro-manipulated probes in a probe station (Figure S3). The translational sensitivity of the probes is 5 μm. Such an instrument allows metal probes to be coated by a conductive paste, which serves as both adhesion and contact points for crystals (Figure 5a and 5b). Although the probe tips are themselves conductive, we found that coating the tips with conductive paste is still necessary for most MOFs. Indeed, in our hands, contacting MOF crystals directly with the probe generally led to either crystal damage or non-ohmic contacts and large contact resistances possibly due to the small contact area between the sharp probe tip (~5 μm in diameter) and the crystal (typically > 40 μm in

diameter). The micro-manipulated probes allow fine control for positioning contacts even on small crystals, with high success rates for the fabrication of 2-contact probe devices with crystals as short as 20 μm .

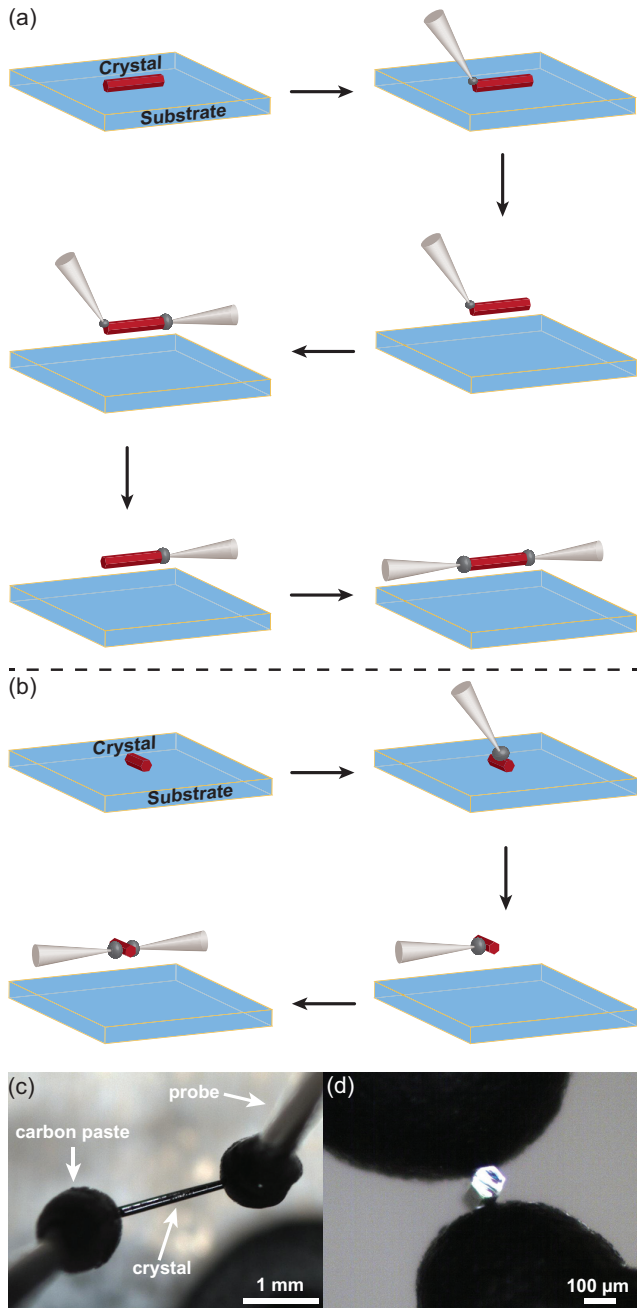


Figure 5. (a, c) Fabrication schematic and optical image of a 2-contact-probe device made from a single crystal of $\text{Cd}_2(\text{TTFTB})$ using the probe-paste approach. The electrical conduction was measured parallel to the crystallographic c axis. (b, d) Fabrication schematic and optical image of a 2-contact-probe device made from a single crystal of $\text{Cd}_2(\text{TTFTB})$ using the probe-paste approach. The electrical conduction was measured perpendicular to the crystallographic c axis.

Because of the fine control afforded by the micro-manipulated probes, we were able to measure the electrical anisotropy

of single crystals of $\text{Cd}_2(\text{TTFTB})$, both parallel and perpendicular to the crystallographic c axis, $\sigma_{\parallel c}$ and $\sigma_{\perp c}$, respectively (Figure 5). Thus, for measuring $\sigma_{\parallel c}$, we used conductive paste to cover the hexagonal ends of crystals, to ensure current passed along the c axis (Figure 5a and 5c). In contrast, for measuring $\sigma_{\perp c}$, we used paste to contact opposite rectangular faces of single crystals (Figure 5b, 5d). Measurements of 5 two-contact-probe single-crystal devices from the same batch of $\text{Cd}_2(\text{TTFTB})$ gave average conductivities $\sigma_{\parallel c} = 9.82 (\pm 2.09) \times 10^{-5} \text{ S/cm}$ and $\sigma_{\perp c} = 2.36 (\pm 0.72) \times 10^{-7} \text{ S/cm}$. We note that the mechanical sensitivity of the single crystals required lifting them from the substrate, made possible by their adherence to the drop of conductive paste covering the probe tip (Figure 5a). A second contact was made with the crystal suspended from the first probe; the measurements thus used air as a substrate. Under these circumstances, we were unable to paste additional probes for obtaining 4-probe devices, primarily because the vibration of the hard tungsten probes led to mechanical failure of the sensitive single crystal devices.

Probe-wire-paste approach

To combine the advantages of the fine control conferred by the micromanipulated probes and address the challenges associated with vibrations, we first connected soft gold wires (25 μm diameter) to the hard tungsten probes, and used the gold wires themselves to contact the crystals, through conductive paste (Figure 6a). The flexible wires eliminate the vibrations associated with evacuating the probe station, necessary to perform measurements in vacuum and at variable temperature. Using this approach, we again fabricated 5 two-contact-probe devices from single crystals of $\text{Cd}_2(\text{TTFTB})$ produced in the same batch (Figure 6b, 6c). These devices gave $\sigma_{\parallel c} = 1.08 (\pm 0.29) \times 10^{-4} \text{ S/cm}$.

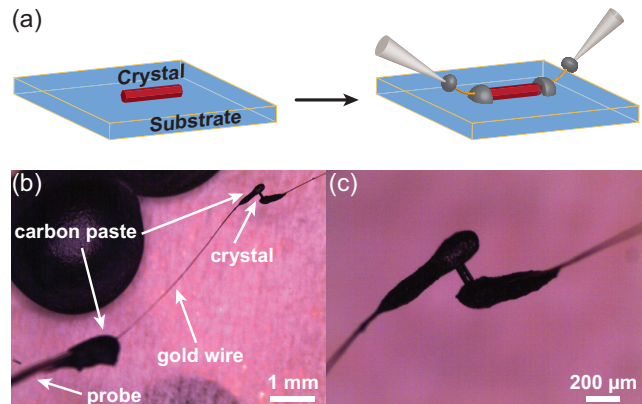


Figure 6. Fabrication schematic and optical images of a 2-contact-probe device made from a single crystal of $\text{Cd}_2(\text{TTFTB})$ using the probe-wire-paste approach.

Other approaches for fabricating single crystal electrical devices of MOFs

In addition to the methods described above, several other approaches may find use in fabricating single crystal devices. These include bottom-contact, top-contact, and alloy approaches. Although we were unable to implement them with crystals of $\text{Cd}_2(\text{TTFTB})$, we hereby provide technical details for completeness.

The bottom-contact approach involves placing a single crystal onto pre-patterned electrodes to fabricate devices (Figure S14). This approach is widely used for fabricating single-crystal field-effect transistors.^{36–38} In principle, this approach could work for very small crystals whose size is limited only by lithography capability. However, because electrodes are in contact with only one crystal surface, charge transport may occur only via this surface, especially if the direction normal to that contacted by electrodes is more insulating, as is the case with Cd₂(TTFB), for instance. In these cases, it is difficult to measure the cross-sectional area of the conduction channel. A detailed discussion can be found in the Supporting Information.

The top-contact approach is widely used for fabricating devices from thin films. It can be adapted to single crystals by covering a crystal with a shadow or lithographic mask exhibiting the desired two- or four-probe pattern. Metal is evaporated onto the crystal and the mask, and removing the mask provides patterned electrode contacts with precise positioning of metallic contacts (Figure S16). Several attempts at producing single crystal devices of Cd₂(TTFB) using this approach were unsuccessful.

In the alloy approach, low-melting Ga-Sn or In-Ga-Sn alloys replace the conductive paste as contacts between wires/probe tips and crystals (Figure S17). Because these alloys do not wet the surface of most materials, crystals can generally be reused, which allows the study of anisotropic electrical properties of the same crystal. Furthermore, unlike the conductive pastes, which are often formulated with organic solvents, the alloys do not dry out upon evacuation, and are therefore particularly useful when performing measurements in vacuum.³⁹ Despite these advantages, we found that both alloys gave only non-ohmic contacts with crystals of Cd₂(TTFB), possibly due to the mismatch between their work functions and that of the MOF, or because the alloys did not wet the crystals sufficiently to enable good contacts.

Comparison and discussion of conductivity data from various techniques

In Figures 7 and S13, we summarize the electrical conductivity of Cd₂(TTFB) obtained from the various methods described previously. From this data, it is clear that the two most important factors affecting the conductivity value, when all external variables are controlled for, are the crystallographic direction and the physical form of the sample. Thus, $\sigma_{\parallel c}$ is higher than $\sigma_{\perp c}$ by 2–3 orders of magnitude, clearly attesting the anisotropy of electrical conductivity in this material, and confirming the TTF stacks, which run parallel to the crystallographic *c* axis, as the major charge transport pathway in Cd₂(TTFB). The anisotropy also suggests that charge hopping between neighboring TTF stacks, which are approximately 19.6 Å apart, is less efficient than within the stacks. Additionally, we find that the electrical conductivity of pressed pellets of Cd₂(TTFB) lies between $\sigma_{\parallel c}$ and $\sigma_{\perp c}$. This is expected and in line with the single crystal studies because crystallites of Cd₂(TTFB) in the pressed pellet are randomly oriented (Figure 3e), and the electrical conductivity of the pellet is the weighted average of the two directions (σ_{average}). Indeed, the pressed pellet conductivity lies closer to $\sigma_{\perp c}$, as expected given that $\sigma_{\perp c}$ corresponds to both *a* and *b* crystallographic directions, and is 2–3 orders of magni-

tude smaller than $\sigma_{\parallel c}$. These results also illustrate how measuring pressed pellets eliminates anisotropy information and in fact tends to underestimate the highest possible conductivity even when grain boundary resistance is minimal. Our results also show that when care is taken to eliminate external variables (e.g. light, atmosphere, temperature), the electrical conductivity values obtained for either single crystals or polycrystalline pellets are consistent across the methods employed, as expected for samples whose conductivity is smaller than the conductivity of the contacts and wires/probes. Finally, we note that the observed electrical conductivity varies by as much as 15-fold even when devices are fabricated by the same approach (wire-paste approach, see Table S2). This significant variance may stem from differences in the quality of crystals and/or devices used in each measurement. Therefore, measuring multiple crystals is necessary to statistically improve the reliability of the observed electrical conductivity of a MOF.

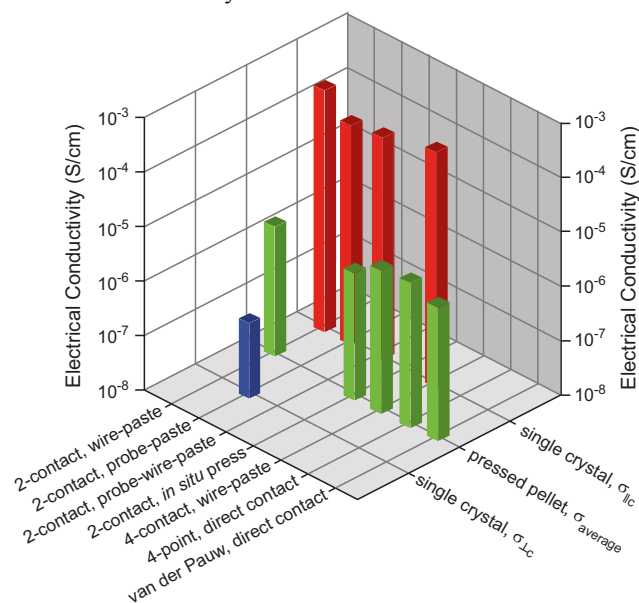


Figure 7. Electrical conductivity data for Cd₂(TTFB).

Influence of environment on electrical conductivity

Having confirmed that the various methods to fabricate electrical devices provide consistent and reproducible results, we tested the influence of the environment on the electrical conductivity of Cd₂(TTFB). It is well known that temperature, pressure, illumination, atmosphere, magnetic field, and electric field may all affect the electrical conductivity of a material. In fact, these effects are the basis of many semiconductor devices, including chemiresistive sensors,⁴⁰ photodiodes,⁴¹ and field-effect transistors,⁴² among others. Therefore, care must be taken when comparing *electrical conductivity values obtained under environmental conditions*. Herein, we demonstrate the influence of temperature, atmosphere, and illumination on the electrical conductivity of single crystals of Cd₂(TTFB). All devices were fabricated by the 2-contact probe method using a wire-paste approach, and values of $\sigma_{\parallel c}$ were compared.

Impact of temperature on the electrical conductivity of Cd₂(TTFB)

The electrical conductivity of metals generally decreases with increasing temperature, whereas the conductivity of semiconductors is thermally activated and typically follows an Arrhenius relationship:

$$\sigma = \sigma_0 \exp\left(-\frac{E_a}{k_B T}\right) \quad (5)$$

where σ_0 is a prefactor, E_a is the activation energy, k_B is the Boltzmann constant, and T is the absolute temperature.⁴³ The larger the activation energy, the more abrupt are the changes in conductivity caused by changes in temperature. For a semiconductor with a large band gap (i.e. large E_a), a small change of temperature may lead to a significant variation of electrical conductivity. Figure 8 shows the change in the electrical conductivity of $\text{Cd}_2(\text{TTFTB})$ in the temperature range 296 to 310 K in air with a relative humidity of 36% ~ 43% and in the absence of light. As T increases from 296 K to 310 K, σ also increases from 8.13×10^{-5} S/cm to 1.36×10^{-4} S/cm, corresponding to an activation energy of 0.293 eV. The slope of the linear increase in conductivity with temperature corresponds to a rate of roughly $3\sim 4 \times 10^{-6}$ S/cm per 1 K. We note here that many literature examples report conductivity at “room temperature”. Our data shows that a two-degree variation in temperature, for instance between 298 K and 300 K, can cause a change of 8×10^{-6} S/cm in conductivity, equivalent to an error of approximately 10%. It is thus imperative that the exact temperature of the electrical measurements be kept constant and that it be reported precisely. Maintaining a constant temperature during electrical measurements is important also because samples may suffer local heating through Ohmic losses, which cause the Seebeck effect that affects electrical signals. These local heating effects must be equilibrated before reading the device resistance; a temperature compensation system should ideally be used for this purpose.

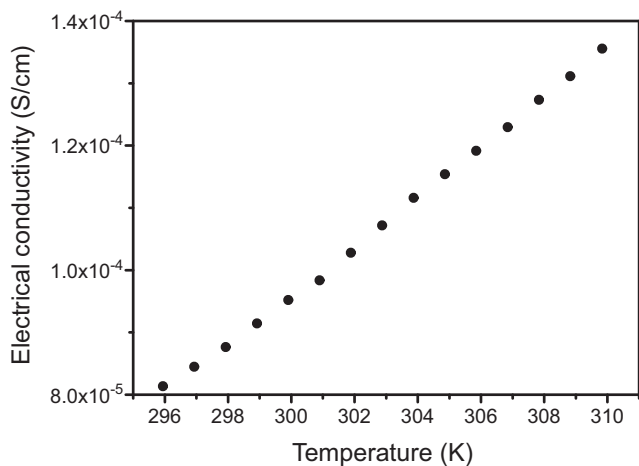


Figure 8. Temperature-activated electrical conduction in a single crystal device made from $\text{Cd}_2(\text{TTFTB})$.

Impact of atmosphere on the electrical conductivity of $\text{Cd}_2(\text{TTFTB})$

Owing to their inherent porosity, MOFs’ electrical conductivity may be greatly affected by the surrounding atmosphere, perhaps more so than other materials. Indeed, guest molecules that are adsorbed by a given MOF may induce chemical, structural,⁴⁴⁻⁴⁶ magnetic,⁴⁷ and optical changes,^{48,49} and could affect electrical conductivity.^{50,51} To test this effect, we evaluated the

electrical response of $\text{Cd}_2(\text{TTFTB})$ to evacuation and air exposure. To do so, we monitored the electrical conductivity of a single crystal of $\text{Cd}_2(\text{TTFTB})$ during 5 consecutive cycles of evacuation and air exposure. The device was kept at 297 K and in the dark. The relative humidity of air was 41%. The conductivity values oscillated between $\sim 1.2 \times 10^{-4}$ S/cm and $\sim 2 \times 10^{-5}$ S/cm in air and vacuum, respectively (Figure 9). Although the absolute conductivity in air decreased by approximately 8% over these 5 cycles, possibly due to incomplete recovery after evacuation or slight device degradation due to the vigorous air flow and rapid evacuation, it was consistently higher than the conductivity in vacuum. The high electrical conductivity in air may originate from either water-induced proton conductivity or oxygen-induced p-type doping. These results illustrate the importance of controlling and reporting the environmental conditions employed for measuring electrical properties, conductivity itself suffering one order of magnitude differences in our devices between air and vacuum. Obviously, the differential response of MOFs in various atmospheres and to different guests may be used for constructing chemiresistive sensor devices^{3,4} or, more fundamentally, to alter or improve electrical or proton conductivity,⁵² to induce host-guest charge transfer interactions,^{50,51} or guest-induced phase changes.⁴⁴⁻⁴⁶

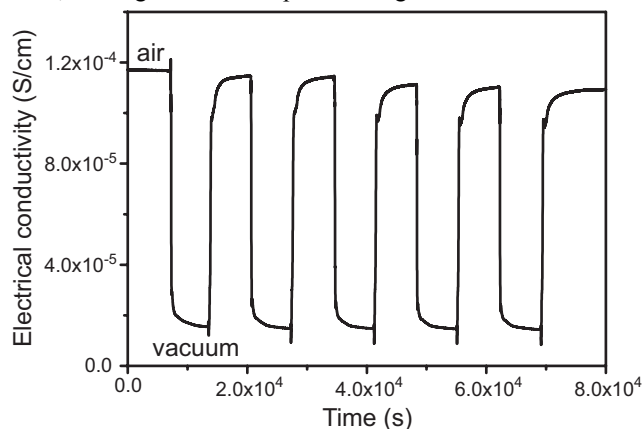


Figure 9. Influence of air and vacuum on the electrical conductivity of single crystal devices made from $\text{Cd}_2(\text{TTFTB})$.

Impact of illumination on the electrical conductivity of $\text{Cd}_2(\text{TTFTB})$

Most semiconductors exhibit photoconductivity, or changes in electrical conductivity upon exposure to electromagnetic radiation (commonly in the visible range). Upon illumination by photons of an appropriate wavelength, electrons in the valence band are excited to the conduction band with a certain probability, thereby forming free charge carriers that improve electrical conductivity.⁵³ We tested the impact of illumination on the electrical conductivity of $\text{Cd}_2(\text{TTFTB})$ by monitoring the electrical response of a single crystal device in the dark and under broadband illumination by a halogen lamp. The device was kept at 297 K, under air with relative humidity of 38%. As shown in Figure 10, under a constant bias of 1 V, the current consistently and reversibly increased under illumination, and decayed in the dark. The increase of current was ~ 350 pA. With photoconductivity studies, heating always accompanies illumination. When electrical conduction is thermally activated, heating obviously will have a positive effect on conductivity. Deconvoluting the effects of heating from those of illumination is difficult. Here,

we observe rapid increase in current (by ~ 325 pA) within 5 s of exposure to light, followed by a slower, more modest increase in current of only 25 pA over the next 25 s. This suggests that the major component of current increase is due to light exposure, not heating, although more detailed studies are required to separate optical and heating effects. To this end, we found that the observed current in $\text{Cd}_2(\text{TTFTB})$ did not change with exposure to ambient light, which is more diffuse and significantly less intense than the halogen lamp. Although it did not affect our material significantly, ambient light is known to have significant impact on more photosensitive materials. Controlling and reporting detailed illumination conditions remains an important consideration when measuring electrical conductivity.

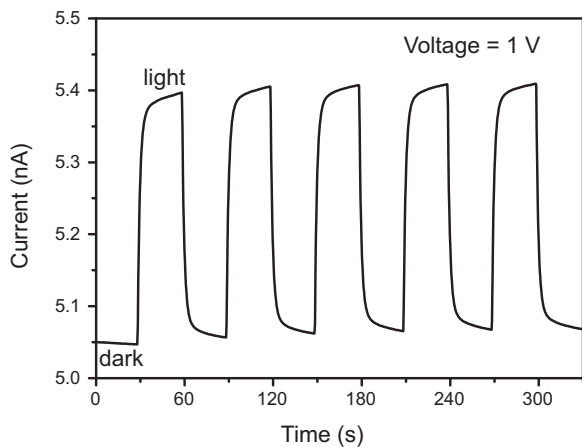


Figure 10. Influence of broadband illumination on the electrical conductivity of single crystal device made from $\text{Cd}_2(\text{TTFTB})$.

Conclusions

We employ the anisotropic MOF $\text{Cd}_2(\text{TTFTB})$ to illustrate several approachable techniques for measuring electrical conductivity in MOFs. We find that sample morphology (i.e. single crystal versus pressed pellet) has a considerable influence on the observed conductivity. Different methods and device fabrication approaches give consistent results as long as external environmental variables are kept constant. Given the variability in pressing pellets and the important influence of crystallite size, we find that single crystal measurements provide more consistent results and are therefore preferable to measuring pressed pellets. Moreover, because they eliminate the effects of contact resistance, 4-probe methods are preferred to 2-probe methods, although the latter is likely sufficiently accurate for more poorly conducting samples with resistances exceeding 1 k Ω . Importantly, with single crystal measurements, we consistently observed significant variations from device to device, and recommend that multiple crystals be measured to obtain average values, which should be reported along with champion devices.

We further show that electrical conductivity is dependent on the environment, as demonstrated for $\text{Cd}_2(\text{TTFTB})$ with temperature, atmosphere, and illumination. In addition to providing a more accurate description of the electrical properties, controlling for these environmental variables is encouraged because it could lead to unusual observations (e.g. crystallographic or magnetic phase changes) and to important applications, such as chemiresistive sensing. Controlling and reporting these varia-

bles with high precision should be required for comparing materials across different research groups. Acceptable standard conditions are 297 K under vacuum or inert atmosphere (N_2 , Ar, or He), and in the dark. Generally, it is advised that complete and detailed information regarding device fabrication, characterization, and raw data processing (i.e. calculation methods) be presented. We have abided by these guidelines in this manuscript, with details on our device fabrication, characterization, and data processing in the Supporting Information.

Following the above, we suggest a “checklist” of experimental conditions that we hope will serve as guidelines for researchers interested in this rapidly developing subclass of MOFs:

- (1) Is the MOF air-sensitive? Was the device fabricated and handled under air-free conditions?
- (2) What is the morphology of the samples used for measurements? Single crystal, pressed pellet, epitaxial film, or polycrystalline film?
- (3) If a single crystal or an epitaxial film was used, which crystallographic direction was measured? Is anisotropy expected given the crystal structure?
- (4) If a pressed pellet was measured, how much pressure was applied? Is the MOF mechanically stable to the applied pressure, as determined by powder X-ray diffraction analysis?
- (5) How many independent batches of the MOF were measured? If applicable, how many crystals were measured in each batch?
- (6) Which method was used to fabricate the device? 2-contact probe, 4-contact probe, 4-point probe, van der Pauw, or another method?
- (7) Are details of the device fabrication provided? These should include information on substrates, electrodes/electrical leads, sample size, contact area, conductive pastes, lithography techniques, deposition methods, special or home-built instruments. Device pictures and/or schematics are desirable.
- (8) Are details on the device characterization provided? These should include the applied voltage/current range, techniques used to measure sample thickness/length/area, exact temperature, atmosphere, optical conditions, electric field, magnetic field, and any other relevant environmental conditions. How were temperature and atmosphere controlled?
- (9) Are details on data processing/calculations provided? These should include tabular and graphical data for the I-V curve and its linear fitting parameters. For the 2-contact and 4-contact probe methods, details on the measurement of the cross sectional area and length should be provided. For the 4-point probe and van der Pauw methods, details on the calculation of the correction factors should be provided.
- (10) How does the MOF respond to external stimuli, such as temperature, pressure, certain chemical, magnetic field, illumination?

ASSOCIATED CONTENT

Supporting Information

Synthesis, crystal indexing, and powder X-ray diffraction of Cd₂(TTFB), details of device fabrication, electrical characterization, and electrical conductivity calculations. This material is available free of charge via the Internet at <http://pubs.acs.org>.

AUTHOR INFORMATION

Corresponding Author

mdinca@mit.edu

ACKNOWLEDGMENT

This work was supported by the U.S. Department of Energy, Office of Science, Office of Basic Energy Sciences, under award no. DE-SC0006937. M.D. thanks the Research Corporation for Science Advancement (Cottrell Scholars) and the Sloan Foundation for non-tenured faculty funds, and the Camille and Henry Dreyfus Foundation for Dreyfus Teacher-Scholar funds. S.S.P. is partially supported by a NSF GRFP (Award No. 1122374). We thank the X-ray laboratory at the Department of Chemistry and Chemical Biology at Harvard University for providing the optical microscope and camera. We thank Dr. Peter Müller for assistance with crystal indexing. Part of the characterization and device fabrication was performed at the Harvard Center for Nanoscale Systems (CNS), a member of the National Nanotechnology Infrastructure Network (NNIN), which is supported by the National Science Foundation under NSF award No. ECS-0335765.

REFERENCES

- (1) Zhou, H.; Long, J. R.; Yaghi, O. M. *Chem. Rev.* **2012**, *112*, 673.
- (2) Stavila, V.; Talin, A. A.; Allendorf, M. D. *Chem. Soc. Rev.* **2014**, *43*, 5994.
- (3) Campbell, M. G.; Sheberla, D.; Liu, S. F.; Swager, T. M.; Dincă, M. *Angew. Chem., Int. Ed.* **2015**, *54*, 4349.
- (4) Campbell, M. G.; Liu, S. F.; Swager, T. M.; Dincă, M. *J. Am. Chem. Soc.* **2015**, *137*, 13780.
- (5) Férey, G.; Millange, F.; Morcrette, M.; Serre, C.; Doublet, M.; Grenèche, J.; Tarascon, J. *Angew. Chem., Int. Ed.* **2007**, *46*, 3259.
- (6) Wiers, B. M.; Foo, M.; Balsara, N. P.; Long, J. R. *J. Am. Chem. Soc.* **2011**, *133*, 14522.
- (7) Zhang, Z.; Yoshikawa, H.; Awaga, K. *J. Am. Chem. Soc.* **2014**, *136*, 16112.
- (8) Aubrey, M. L.; Long, J. R. *J. Am. Chem. Soc.* **2015**, *137*, 13594.
- (9) Zhang, Z.; Yoshikawa, H.; Awaga, K. *Chem. Mater.* **2016**, *28*, 1298.
- (10) Choi, K. M.; Jeong, H. M.; Park, J. H.; Zhang, Y.; Kang, J. K.; Yaghi, O. M. *ACS Nano* **2014**, *8*, 7451.
- (11) Sheberla, D.; Bachman, J. C.; Elias, J. S.; Sun, C.; Shao-Horn, Y.; Dincă, M. *Nat. Mater.* **2016**, DOI: 10.1038/nmat4766.
- (12) Liu, J.; Zhou, W.; Liu, J.; Howard, I.; Kilibarda, G.; Schlabach, S.; Coupry, D.; Addicoat, M.; Yoneda, S.; Tsutsui, Y.; Sakurai, T.; Seki, S.; Wang, Z.; Lindemann, P.; Redel, E.; Heine, T.; Wöll, C. *Angew. Chem., Int. Ed.* **2015**, *54*, 7441.
- (13) Erickson, K. J.; Léonard, F.; Stavila, V.; Foster, M. E.; Spataru, C. D.; Jones, R. E.; Foley, B. M.; Hopkins, P. E.; Allendorf, M. D.; Talin, A. A. *Adv. Mater.* **2015**, *27*, 3453.
- (14) Panda, T.; Banerjee, R. *Proc. Natl. Acad. Sci. India Sect. A Phys. Sci.* **2014**, *84*, 331.
- (15) Huang, X.; Sheng, P.; Tu, Z.; Zhang, F.; Wang, J.; Geng, H.; Zou, Y.; Di, C.; Yi, Y.; Sun, Y.; Xu, W.; Zhu, D. *Nat. Commun.* **2015**, *6*, 7408.
- (16) Suh, M. P.; Park, H. J.; Prasad, T. K.; Lim, D. *Chem. Rev.* **2012**, *112*, 782.
- (17) Sumida, K.; Rogow, D. L.; Mason, J. A.; McDonald, T. M.; Bloch, E. D.; Herm, Z. R.; Bae, T. H.; Long, J. R. *Chem. Rev.* **2012**, *112*, 724.
- (18) Li, J.; Sculley, J.; Zhou, H. *Chem. Rev.* **2012**, *112*, 869.
- (19) Lee, J.; Farha, O. K.; Roberts, J.; Scheidt, K. A.; Nguyen, S. T.; Hupp, J. T. *Chem. Soc. Rev.* **2009**, *38*, 1450.
- (20) Yoon, M.; Srirambalaji, R.; Kim, K. *Chem. Rev.* **2012**, *112*, 1196.
- (21) Kreno, L. E.; Leong, K.; Farha, O. K.; Allendorf, M. D.; Van Duyn, R. P.; Hupp, J. T. *Chem. Rev.* **2012**, *112*, 1105.
- (22) Sun, L.; Campbell, M. G.; Dincă, M. *Angew. Chem., Int. Ed.* **2016**, *55*, 3566.
- (23) Park, S. S.; Hontz, E. R.; Sun, L.; Hendon, C. H.; Walsh, A.; Van Voorhis, T.; Dincă, M. *J. Am. Chem. Soc.* **2015**, *137*, 1774.
- (24) Franssila, S. *Introduction to Microfabrication*, 2nd ed.; Wiley: Chichester, United Kingdom, 2010.
- (25) Zhang, Z.; Jin, C.; Liang, X.; Chen, Q.; Peng, L. *Appl. Phys. Lett.* **2006**, *88*, 73102.
- (26) Lampert, M. A.; Mark, P. In *Current Injection in Solids*; Academic Press: New York, United States of America, 1970; pp 112–138.
- (27) Schroder, D. K. In *Semiconductor Material and Device Characterization*; Wiley: Hoboken, United States of America, 2006; pp 1–60.
- (28) Roth, S.; Carroll, D. In *One-Dimensional Metals: Conjugated Polymers, Organic Crystals, Carbon Nanotubes and Graphene*; Wiley-VCH: Weinheim, Germany, 2015; pp 159–208.
- (29) van der Pauw, L. J. *Philips Res. Reports* **1958**, *13*, 1.
- (30) van der Pauw, L. J. *Philips Tech. Rev.* **1958**, *20*, 220.
- (31) Wudl, F.; Bryce, M. R. *J. Chem. Educ.* **1990**, *67*, 717.
- (32) Kambe, T.; Sakamoto, R.; Hoshiko, K.; Takada, K.; Miyachi, M.; Ryu, J.; Sasaki, S.; Kim, J.; Nakazato, K.; Takata, M.; Nishihara, H. *J. Am. Chem. Soc.* **2013**, *135*, 2462.
- (33) Kambe, T.; Sakamoto, R.; Kusamoto, T.; Pal, T.; Fukui, N.; Hoshiko, K.; Shimojima, T.; Wang, Z.; Hirahara, T.; Ishizaka, K.; Hasegawa, S.; Liu, F.; Nishihara, H. *J. Am. Chem. Soc.* **2014**, *136*, 14357.
- (34) Sheberla, D.; Sun, L.; Blood-Forsythe, M. A.; Er, S.; Wade, C. R.; Brozek, C. K.; Aspuru-Guzik, A.; Dincă, M. *J. Am. Chem. Soc.* **2014**, *136*, 8859.
- (35) Rhoderick, E. H.; Williams, R. H. *Metal-Semiconductor Contacts*, 2nd ed.; Oxford University Press: New York, United States of America, 1988.
- (36) Menard, E.; Podzorov, V.; Hur, S.; Gaur, A.; Gershenson, M. E.; Rogers, J. A. *Adv. Mater.* **2004**, *16*, 2097.
- (37) Kang, S. J.; Kim, B.; Kim, K. S.; Zhao, Y.; Chen, Z.; Lee, G. H.; Hone, J.; Kim, P.; Nuckolls, C. *Adv. Mater.* **2011**, *23*, 3531.
- (38) Xie, W.; Wang, S.; Zhang, X.; Leighton, C.; Frisbie, C. D. *Phys. Rev. Lett.* **2014**, *113*, 246602.
- (39) *Keithley Application Note No.2464*.
- (40) Chiu, S.; Tang, K. *Sensors* **2013**, *13*, 14214.
- (41) Baeg, K.; Binda, M.; Natali, D.; Caironi, M.; Noh, Y. *Adv. Mater.* **2013**, *25*, 4267.
- (42) Grosso, G.; Pastori Parravicini, G. In *Solid State Physics*; Academic Press: Amsterdam, Netherland, 2014; pp 609–642.
- (43) Grosso, G.; Pastori Parravicini, G. In *Solid State Physics*; Academic Press: Amsterdam, Netherland, 2014; pp 577–608.
- (44) Barthelet, K.; Marrot, J.; Riou, D.; Férey, G. *Angew. Chem., Int. Ed.* **2002**, *41*, 281.
- (45) Murdock, C. R.; Hughes, B. C.; Lu, Z.; Jenkins, D. M. *Coord. Chem. Rev.* **2014**, *258–259*, 119.
- (46) Sun, L.; Hendon, C. H.; Minier, M. A.; Walsh, A.; Dincă, M. *J. Am. Chem. Soc.* **2015**, *137*, 6164.
- (47) Bao, X.; Shepherd, H. J.; Salmon, L.; Molnár, G.; Tong, M.; Bousseksou, A. *Angew. Chem., Int. Ed.* **2013**, *52*, 1198.
- (48) Allendorf, M. D.; Bauer, C. A.; Bhakta, R. K.; Houk, R. J. T. *Chem. Soc. Rev.* **2009**, *38*, 1330.
- (49) Shustova, N. B.; McCarthy, B. D.; Dincă, M. *J. Am. Chem. Soc.* **2011**, *133*, 20126.
- (50) Kobayashi, Y.; Jacobs, B.; Allendorf, M. D.; Long, J. R. *Chem. Mater.* **2010**, *22*, 4120.
- (51) Talin, A. A.; Centrone, A.; Ford, A. C.; Foster, M. E.; Stavila, V.; Haney, P.; Kinney, R. A.; Szalai, V.; El Gabaly, F.; Yoon, H. P.; Léonard, F.; Allendorf, M. D. *Science* **2014**, *343*, 66.
- (52) Ramaswamy, P.; Wong, N. E.; Shimizu, G. K. H. *Chem. Soc. Rev.* **2014**, *43*, 5913.
- (53) Grosso, G.; Pastori Parravicini, G. In *Solid State Physics*; Academic Press: Amsterdam, Netherland, 2014; pp 529–576.

Insert Table of Contents artwork here

